method has been used by Kwok & Evans (1981) to measure the elastic area compressibility of a single EPC bilayer. An interesting result was that the elastic area compressibility of the single bilayer was nearly the same as the value deduced from analysis of equilibrium dehydration of multilayers in the range of partial hydration (Evans & Skalak, 1979). This indicates that the surface compressibility was essentially unaffected by proximity of the bilayers. If the lipid diffusivity depends only on area per molecule to the extent shown in Figure 7, we would anticipate about a 20–30% increase in diffusivity for a 3–4% area dilation (which is the limit where the vesicles are typically lysed). We are presently pursuing this study.

The important conclusion is that the lateral diffusivity in multibilayer systems is a strong function of the activity of the water phase, or water content, even though the acyl chains remain in the fluid state. It is expected that this property will significantly affect the kinetics of processes that involve membrane–membrane contact, e.g., fusion and vesiculation events.

References

Axelrod, D., Koppel, D. E., Schlessinger, J., & Elson, E. (1976) *Biophys. J. 16*, 1055.
Barrett, J. J., & Adams, N. I. (1968) *J. Opt. Soc. Am. 58*, 311.
Dickson, L. D. (1970) *Appl. Opt. 9*, 1854.
Elworthy, P. H. (1961) *J. Chem. Soc.*, 5385.
Evans, E. A., & Skalak, R. (1979) *CRC Crit. Rev. Bioeng. 4*, 380.
Fahey, P. F., & Webb, W. W. (1978) *Biochemistry 17*, 3046.
Gary-Bobo, C. M., & Rigand, J. L. (1975) *Colloq. Int. C.N.R.S. 246*, 121.
Jacobson, K., Derzko, Z., Wu, E.-S., Hou, Y., & Poste, G. (1976) *J. Supramol. Struct. 5*, 565 (417).
Kwok, R., & Evans, E. (1981) *Biophys. J.* (in press).
LeNeveu, D. M., Rand, R. P., Parsegian, V. A., & Ginell, D. (1977) *Biophys J. 18*, 209.
Liu, N.-I., & Kay, R. L. (1977) *Biochemistry 16*, 3484.
Lundberg, B., Svens, E., & Ekman, S. (1978) *Chem. Phys. Lipids 22*, 285.
Owicki, J. C., & McConnell, H. M. (1980) *Biophys. J. 30*, 383.
Parsegian, V. A., Fuller, N., & Rand, R. P. (1979) *Proc. Natl. Acad. Sci. U.S.A. 76*, 2750.
Powers, L., & Pershan, P. S. (1977) *Biophys. J. 20*, 137.
Reiss-Husson, F. (1967) *J. Mol. Biol. 25*, 363.
Rubenstein, J. L. R., Smith, B. A., & McConnell, H. M. (1978) *Proc. Natl. Acad. Sci. U.S.A. 76*, 15.
Small, D. (1967) *J. Lipid Res. 8*, 551.
Smith, B. A., & McConnell, H. M. (1978) *Proc. Natl. Acad. Sci. U.S.A. 75*, 2759.
Wu, E.-S., Jacobson, K., & Papahadjopoulos, D. (1977) *Biochemistry 16*, 3936.
Wu, E.-S., Jacobson, K., Szoka, F., & Portis, A. (1978) *Biochemistry 17*, 5543.
Van Deenen, L. L. M., Houtsmuller, U. M. T., DeHaas, G. H., & Mulder, E. (1962) *J. Pharm. Pharmacol. 14*, 429.
Vaz, W. L. C., Jacobson, K., Wu, E.-S., & Derzko, Z. (1979) *Proc. Natl. Acad. Sci. U.S.A. 76*, 5645.

Characterization by Infrared Spectroscopy of the Bilayer to Nonbilayer Phase Transition of Phosphatidylethanolamines†

Henry H. Mantsch,* Adèle Martin, and David G. Cameron

ABSTRACT: A Fourier-transform infrared spectroscopic study of the thermotropic behavior of egg yolk phosphatidylethanolamines is reported. Two phase changes were monitored, the gel to liquid-crystalline acyl chain melting transition, centered at 12 °C, and a transition from the liquid-crystalline to the inverted hexagonal phase, centered at 28 °C. It is demonstrated that the gel to liquid-crystalline phase transition results in a large increase in the conformational disorder of the acyl chains in the bilayer and that the nonbilayer phase contains a still higher degree of conformational disorder. It is shown that the transition to the inverted hexagonal phase is promoted by highly unsaturated acyl chains. A model is developed for the bilayer to nonbilayer phase transition in which it is proposed that the driving force which triggers this phase transition is the introduction of a degree of conformational disorder so high that the integrity of the bilayer surface can no longer be maintained, due to the volume requirements of the acyl chains. A number of previously reported data are rationalized in terms of this hypothesis.

The physical properties of lipids provide information of fundamental significance to the determination of the structural and functional properties of biomembranes. With this aspect in mind, there have been numerous physical studies of lipid bilayer structures in the gel phase (Figure 1A) and in the liquid-crystalline phase (Figure 1B). However, there are certain naturally occurring lipids, particularly the phosphatidylethanolamines, which also form nonbilayer structures, such as the inverted hexagonal (H_{II}) phase (Figure 1C). The macromolecular properties of this H_{II} phase have been well characterized by differential scanning calorimetry (Cullis & de Kruiff, 1978) and by X-ray (Luzatti et al., 1968; Rand et al., 1971) and freeze–fracture techniques (Cullis et al., 1978a). However, studies employing spectroscopic methods capable of monitoring the molecular properties have been so far limited to ^{31}P NMR (Cullis & de Kruiff, 1976, 1978) and ^{2}H NMR (Gally et al., 1980; Taylor & Smith, 1981). The nature and particularly the driving force of the transition from the lamellar

† From the Division of Chemistry, National Research Council of Canada, K1A 0R6, Ottawa, Canada. *Received October 21, 1980.* Issued as NRCC No. 18867.

0006-2960/81/0420-3138$01.25/0

Table I: Fatty Acid Composition (% Weight) of the Natural and the Semisynthetic Phosphatidylethanolamine

phospholipid	16:0	16:1	18:0	18:1	18:2	20:4	22:6	others
natural PE	20.2		27.5	17.2	7.5		16.9	4.5
semisynthetic PE (from PC)	36.7	1.2	12.7	31.6	15.4			1.9

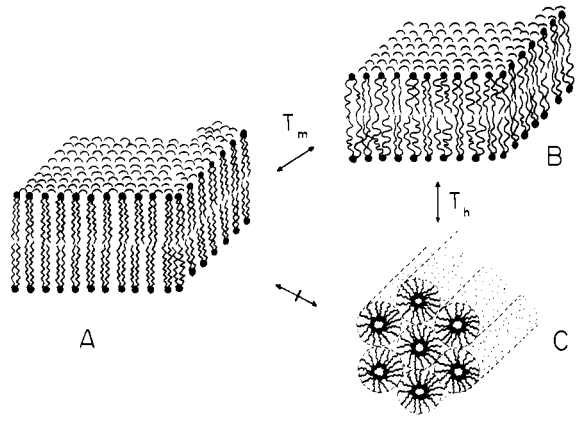

FIGURE 1: Pictorial description of the lamellar bilayer structures in the gel phase (A) or in the liquid-crystalline phase (B) and of the hexagonal nonbilayer structure (C). T_m (m for melting) and T_h (h for hexagonal) indicate the corresponding phase transitions.

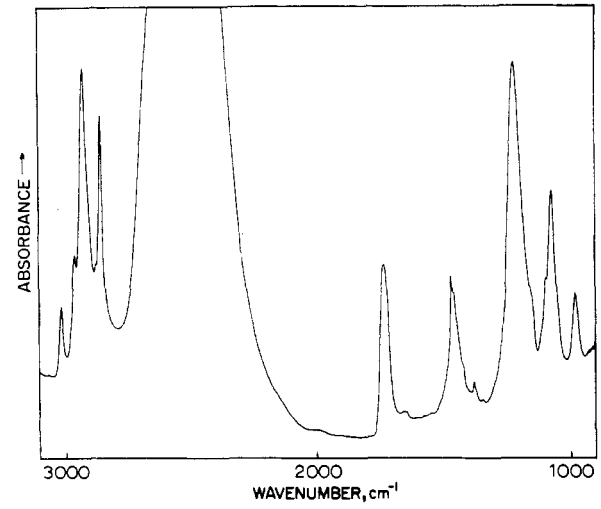

FIGURE 2: Fourier-transform infrared spectrum of hen egg yolk PE multibilayers in the gel phase at 5 °C in the presence of excess water (D_2O).

to a nonlamellar phase are not yet fully understood.

In the present investigation, we demonstrate the applicability of the Fourier-transform infrared spectroscopic technique to the study of several aspects of the thermal behavior of natural phosphatidylethanolamines. While infrared spectroscopy per se cannot be used to identify absolutely a certain phase, it does permit the precise monitoring of subtle changes in absorption bands characteristic of specific functional groups. Using such data, in combination with the mascroscopic structures obtained from X-ray and freeze–fracture techniques (Cullis & de Kruiff, 1979), we suggest a mechanism of the bilayer to nonbilayer phase transition in which the conformational disorder of the acyl chains is the driving force behind this transition.

Experimental Procedures

Materials. Natural hen egg yolk phosphatidylethanolamine (PE)[1] was purchased from Lipid Products (South Nutfield, UK). The semisynthetic PE was prepared from hen egg yolk phosphatidylcholine (Sigma) by a transesterification reaction employing cabbage phospholipase D (Calbiochem) and ethanolamine (Fisher), according to the method of Yang et al. (1967) as modified by Seelig & Gally (1976). Both phosphatidylethanolamines were purified on a silicic acid column by using chloroform with increasing amounts (from 3% to 50%) of methanol. The fatty acid composition is given in Table I.

Spectra. Thin films of multilamellar dispersions of egg yolk phosphatidylethanolamines were prepared for infrared spectroscopy according to the detailed methods reported earlier (Cameron et al., 1979, 1980). Freshly purified PE samples were hydrated with double-distilled H_2O or with 99.7% D_2O; 6-μm thick cells with BaF_2 or CaF_2 windows were used. Spectra were recorded with a Digilab FTS-11 Fourier-transform spectrometer equipped with a mercury cadmium telluride detector (Infrared Associates, New Brunswick, NJ) and a 3900-cm^{-1} high-frequency cutoff filter. Six hundred scans were accumulated and co-added, using a maximum optical retardation of 1 cm and a moving mirror velocity of 1.2 cm s^{-1} (collection rate ~50 scans/min). The resultant interferograms were triangularly apodized and Fourier transformed with one level of zero filling to yield a resolution of 0.9 cm^{-1} and an encoding interval of 0.45 cm^{-1}.

For temperature regulation, the cell was placed in a hollow cell mount thermostated by a flow of ethanol/water, which gives a temperature stability of better than 0.1 °C. The temperature was monitored by a copper–constantan thermocouple located against the cell window, a continuous record being obtained on a printer via a Newport digital pyrometer. The spectrometer controlled the complete operation of recording a spectrum, printing and incrementing the temperature, waiting for temperature equilibration, and then repeating the sequence. Throughout a sequence of measurements (usually from 4 to 45 °C), the sample remained totally untouched; the only operational parameter which varied was the temperature. We find no evidence for sample degradation under these conditions, and thin-layer chromatography showed identical traces before and after the experiment. Furthermore, after the sample was cooled to 4 °C, we were able to reproduce for a second and a third time all temperature-induced changes previously observed by repeating the heating cycle from 4 to 45 °C.

Difference spectra were recorded and processed according to the techniques described in detail elsewhere (Cameron et al., 1980); neither the absorbance nor the difference spectra were smoothed. Frequencies were measured by determining the center of area of the top five (C–H modes) or nine (C=O mode) data points of the peak (Kauppinen et al., 1978), a most precise method for determining the frequency of the maximum position of an absorbance band contour. In combination with the signal-to-noise ratio employed in this study, temperature-induced frequency shifts of 0.1 cm^{-1} could be determined and reproduced from one measurement to another. Bandwidths and integrated intensities were measured by digitally subtracting a linearly interpolated base line and computing

[1] Abbreviations used: PE, phosphatidylethanolamine; PC, phosphatidylcholine; PS, phosphatidylserine; T_m, gel to liquid-crystalline acyl chain melting phase transition; T_h, bilayer to inverted hexagonal phase transition.

Table II: Assignments for the Main Bands in the Infrared Spectrum of Hydrated Multibilayers of Egg Yolk Phosphatidylethanolamine in the Gel Phase

frequency (cm^{-1})	relative[a] intensity	tentative[b] assignment
3012	m	=C–H stretch
2956	s	asymmetric CH_3 stretch
2919	vs	antisymmetric CH_2 stretch
2875	sh	symmetric CH_3 stretch
2851	vs	symmetric CH_2 stretch
2700, 2300	vs	O–D stretch (D_2O)
1738	s	C=O stretch
1468	s	CH_2 scissoring
1378	w	CH_3 bending
1345	w	CH_2 wagging
1219	vs	asymmetric PO_2 stretch + O–D deformation (D_2O)
1094	sh	symmetric PO_2 stretch
1071	s	C–O–C stretch
981	m	C–C–N^+ stretch

[a] vs, very strong; s, strong; m, medium; w, weak; sh, shoulder. [b] See Akutsu et al. (1975) and Fookson & Wallach (1978).

the width at a selected fraction of the peak height for a given band.

Results

Figure 2 shows the infrared spectrum of fully hydrated multilamellar egg yolk PE in the gel phase at 5 °C. Despite the complexity of the head group and the inhomogeneity of the acyl chains, the infrared spectrum is surprisingly simple. A large excess of water (D_2O) is evident from the strong infrared absorption in the O–D stretching region (2700–2300 cm^{-1}). The frequencies and assignments of the principal bands are given in Table II. They fall into two classes: those resulting from head group vibrations (the ethanolamine, the phosphate, and the ester groups) and those resulting from the acyl chains. The latter category can be further subdivided into bands resulting from the terminal methyl groups, the CH=CH groups, and all the methylene groups. The vibrational modes are essentially decoupled from each other; hence, the changes in the infrared spectra yield discrete information regarding each of these functional groups.

In order to study the temperature-dependent phase behavior of egg yolk PE, a series of spectra was recorded at temperatures encompassing the phase transitions T_m and T_h. A first analysis of these raw spectral data was obtained by deriving a series of difference spectra. Such a difference spectrum, the result of subtracting an absorbance spectrum (A_{T-1}) from that recorded at the next highest temperature (A_T), contains nonzero values only in those regions where the temperature variation has resulted in a change in the band contour.

Figure 3 shows a series of infrared difference spectra resulting from the stretching bands of the C=O, the CH_2, and the =C—H groups and from the scissoring band of the CH_2 group. Each series of difference spectra shows two discrete temperature ranges within which the spectra change rapidly, providing evidence of two phase transitions in this system. The midpoints of these temperature ranges coincide with the two maxima in the differential scanning calorimetric traces of egg yolk PE (Cullis & de Kruiff, 1978). Hence, we may conclude that these spectral changes reflect the transitions between the three phases (A, B, and C in Figure 1), which have been previously characterized by X-ray and freeze–fracture techniques (Cullis & de Kruiff, 1979). The transition occurring at lower temperatures is ramplike in that the rate of change increases gradually with temperature and is greatest at temperatures immediately preceding the abrupt cessation of the phase transition. This ramplike feature is characteristic of the acyl chain melting phase transition (Casal et al., 1980). In contrast, the higher temperature phase transition has a symmetric shape, the rate of change being greatest in the center of the transition temperature range.

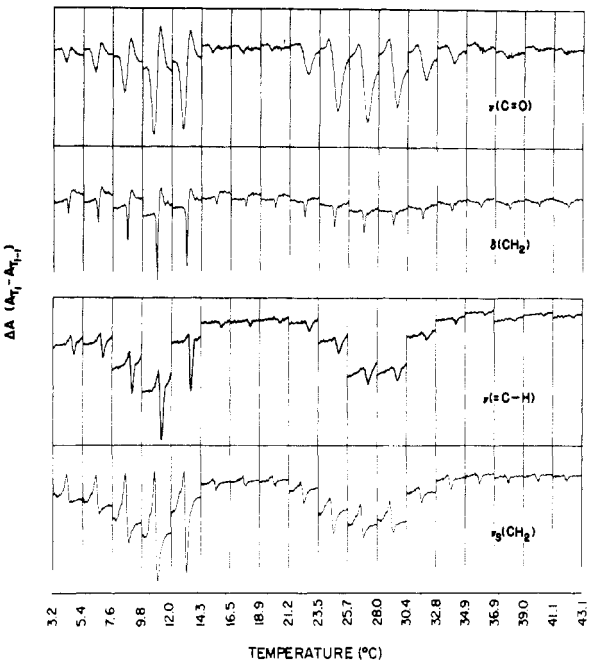

FIGURE 3: Infrared difference spectra in the regions 3080–2980, 2900–2800, 1780–1680, and 1520–1420 cm^{-1} corresponding respectively to the vibrational modes ν (=CH), ν_s (CH_2), ν (C=O), and δ (CH_2).

Table III: Frequencies of Selected Absorption Bands of PE in the Gel Phase (5 °C), the Liquid-Crystalline Phase (19 °C), and the Inverted Hexagonal Phase (39 °C) in D_2O

band	frequency (cm^{-1}) 5 °C	19 °C	39 °C
ν (=CH)	3012.1	3012.9	3013.5
ν_{as} (CH_3)	2955.9	2956.3	2957.0
ν_{as} (CH_2)	2918.5	2921.4	2922.8
ν_s (CH_2)	2850.4	2852.6	2853.6
ν (C=O)	1737.7	1733.6	1737.7
CH_2 scissoring	1468.4	1467.3	1466.1
CH_3 bend	1377.7	1378.0	1377.7
CH_2 wag	1344.9	1344.9	1345.0
ν (COC)	1070.6	1071.9	1072.5
ν (CCN)	981.0	981.0	981.0

These changes are, of course, also reflected in the actual absorbance band contours, two of which are shown in Figure 4. In the case of the symmetric CH_2 stretching band (Figure 4A), the trend most evident with an increase in temperature is a shift to higher frequency. Maximum rates of change are evident in two temperature ranges; outside these ranges the spectra superimpose, demonstrating the lack of further changes. The carbonyl stretching band (Figure 4B) also exhibits two regions of maximal change; the first transition results in a shift of the band maximum to lower frequencies, while the second transition reverses this frequency shift. Furthermore, variations in band symmetry and width are also evident and will be discussed later.

In addition to the bands discussed above, changes were observed in several other bands, and, of equal significance, lack of change was found in some bands. These data are summarized in Table III, which gives the frequencies at 5, 19, and 39 °C, i.e., at temperatures which bracket the two phase

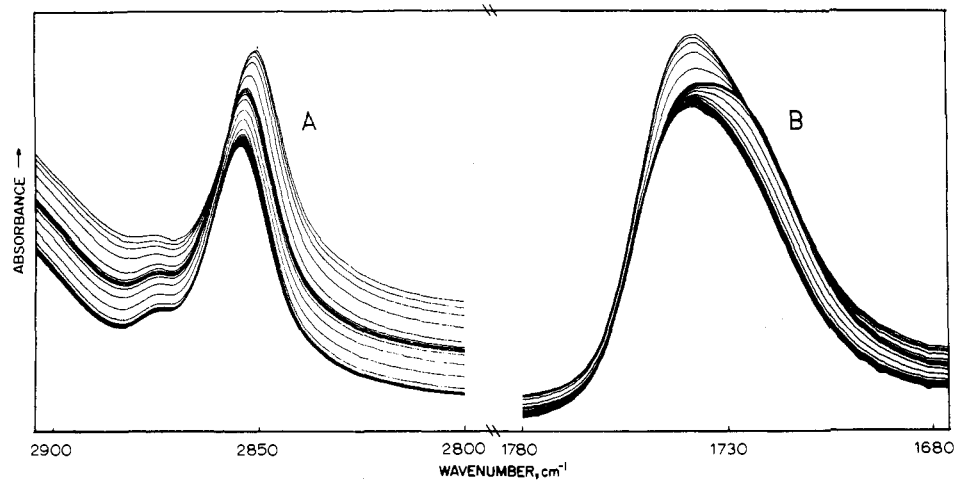

FIGURE 4: Temperature-dependent behavior of the symmetric CH_2 stretching (A) and of the C=O stretching band (B). The top spectrum is at 3.2 °C and the bottom spectrum at 43.1 °C. There are 20 individual spectra, each about 2 °C apart.

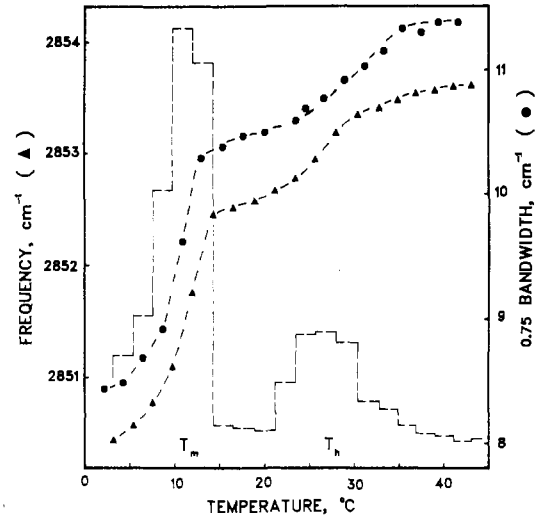

FIGURE 5: Temperature profiles of the symmetric CH_2 stretching vibration between 4 and 45 °C.

transitions and thus are characteristic for structures A, B, and C in Figure 1.

Acyl Chain Bands. Details of the thermotropic behavior of the symmetric CH_2 stretching band are given in Figure 5. The broken line is a plot of $\Delta A/\Delta T$ vs. temperature derived from the difference spectra in Figure 3 by normalizing ΔA with respect to the corresponding temperature increment (Mantsch et al., 1980). Superimposed are plots of the temperature dependence of the frequency and bandwidth. These temperature profiles show that the $\Delta A/\Delta T$ plot results from changes in bandwidth and frequency, thus providing a good parameter for monitoring the overall rate of change of this band as a function of temperature. In the temperature range 4 to 14 °C, the frequency shifts from 2850.4 to 2852.6 cm^{-1} and is accompanied by a 20% increase in bandwidth. The combination of these changes is typical of an acyl chain melting phase transition and results from the introduction of a high population of gauche conformers (Cameron et al., 1980). The increase in conformational disorder is also evident in the decrease in intensity of the 1468-cm^{-1} band, which gives rise to the narrow negative bands at this frequency in the difference spectra in Figure 3.

In the range 14–22 °C, the liquid-crystalline phase is stable and only slight increases in bandwidth and frequency are evident in Figure 5. At 22 °C, the transition to the inverted hexagonal phase commences and continues to about 35 °C. Within this temperature range, an additional shift in frequency of about 1 cm^{-1} is observed. This is accompanied by a 10% increase in bandwidth, indicating that additional conformational disorder is introduced by this transition. Confirmation of this conclusion comes from the further decrease in the intensity of the CH_2 scissoring band at 1468 cm^{-1} (Figure 3).

Three other CH stretching bands, resulting from CH_2 [ν_{as} (CH_2)], CH_3 [ν_{as} (CH_3)], and HC=CH [ν (=CH)] groups, were also monitored. In all cases, the relative magnitudes of the changes at the two transitions were similar, supporting the conclusions derived from the symmetric CH_2 stretching band. The plots are identical in form with that in Figure 5 and are not shown.

Head-Group Bands. As shown in Table III, the bands resulting from the phosphate and ethanolamine groups are rather insensitive to both phase changes whereas those resulting from the ester linkages show large changes both at T_m and T_h. The temperature profiles derived from the ester group C=O and C–O absorption bands show the same general form; therefore, we restrict the discussion to the C=O stretching band which does not suffer from overlap with other bands. The temperature profiles derived from this band are given in Figure 6. The $\Delta A/\Delta T$ plot identifies the two temperature intervals within which there is an increased overall rate of change and which define T_m and T_h. Again, the symmetric shape of T_h contrasts with the ramplike shape of the acyl chain melting transition T_m. Neither of these two transitions is very sharp; T_m occurs over a temperature range of about 10 °C, while T_h covers a range of about 13 °C.

The frequency plot in Figure 6 quantitates the qualitative trends reflected in the difference (Figure 3) and absorbance spectra (Figure 4B). The frequencies of the C=O band maxima of the bilayer gel phase and of the inverted hexagonal phase are nearly identical whereas that of the bilayer in the liquid-crystalline phase is 3.5 cm^{-1} lower in frequency.

The bandwidth and intensity of the C=O stretching band also exhibit large changes with temperature. As in the case of the frequencies, the bandwidths are nearly identical in the gel-phase bilayer and in the inverted hexagonal phase, while a substantially different value is observed for the bilayer in the liquid-crystalline phase. Both phase changes result in a decrease in integrated intensity (a total decrease of about 12%), the larger decrease being observed at T_h. The complexity of the changes in this band contour results partly from the fact that it is comprised of two components; consequently, the frequencies and bandwidths shown in Figure 6 result from the sum of two overlapping bands. We have recently developed a Fourier deconvolution (not to be confused with curve-fitting)

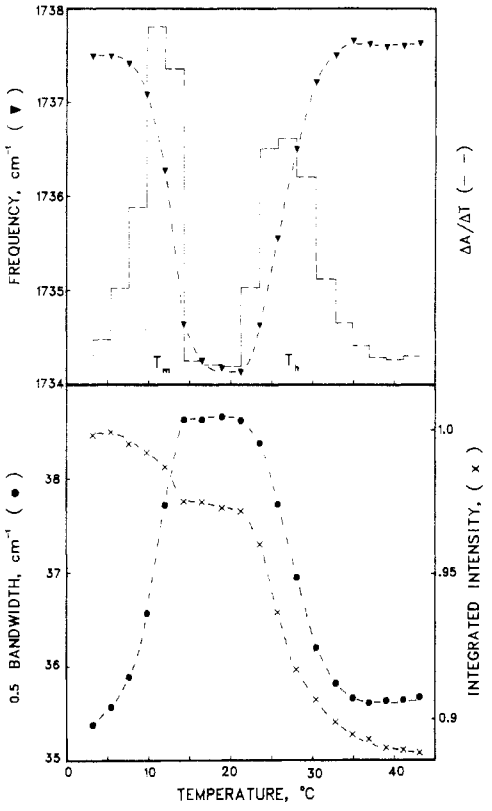

FIGURE 6: Temperature induced changes in the IR spectral parameters of the C=O stretching vibration.

technique (Kauppinen et al., 1981) which allowed the recovery of the two main component bands at 1743 and 1726 cm^{-1}. These values are in good agreement with the values of 1741 and 1721 cm^{-1} which Bush et al. (1980) have assigned respectively to the *sn*-1 and *sn*-2 carbonyls in dipalmitoyl-PC. The frequencies of the two deconvoluted C=O bands in PE are almost invariant with temperature; however, the relative peak heights vary substantially and thus result in the changes in the spectral parameters shown in Figure 6. The change in integrated intensity can be attributed partly to changes in density as a result of the structural rearrangements which accompany both phase transitions. Such density changes, however, will not affect the frequency or bandwidth. The overall changes observed at T_m are similar in magnitude and direction to those observed for the C=O band of phosphatidylcholine bilayers at the gel to liquid-crystalline phase transition (Umemura et al., 1980); however, at T_h, on transition to the inverted hexagonal phase, the overall band shape and the relative intensities of the two components revert to those observed in the gel phase. The two deconvoluted peaks at 1743 and 1726 cm^{-1} do not shift in frequency either at T_m or at T_h.

Discussion

As demonstrated throughout the preceding section, the phase transitions T_m and T_h can be precisely monitored by infrared spectroscopy. Furthermore, because of the nature of the infrared technique, it is possible to monitor these transitions via a number of functional groups and to observe differences in their thermotropic behavior. Since these groups are located at discrete positions in the PE molecules, they probe structural changes at different sites of the molecule. In this respect the functional groups may be divided into two catagories. First, there are the bands originating from the phosphate and the ethanolamine groups, which are almost invariant with temperature; this indicates that the conformations and the degree

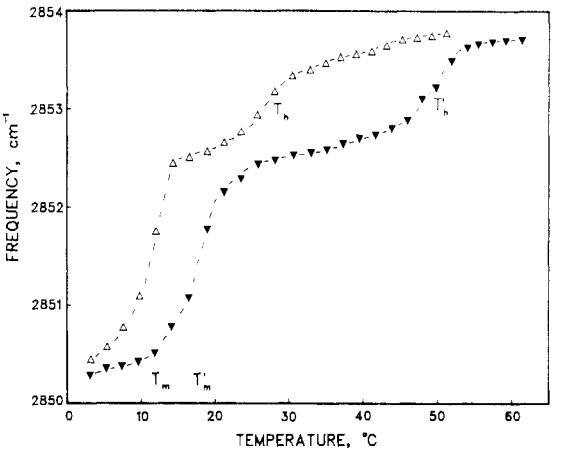

FIGURE 7: Temperature dependence of the frequency of the symmetric CH_2 stretching vibration in natural egg yolk PE (Δ) and in PE obtained from egg yolk PC (▼).

of hydrogen bonding of the functional groups located in the head-group region are similar in all phases. The second category encompasses those functional groups whose spectral characteristics are drastically altered by the two phase transitions. These include the bands originating from the methyl, the methylene, and the CH=CH groups, all part of the acyl chains, as well as those originating from the ester linkage, i.e., the C=O and C–O bands.

The changes observed in the acyl chain bands at T_h are very similar to those observed at T_m, but smaller in magnitude. We have previously characterized the changes of the infrared spectral parameters at T_m for various lipids (Casal et al., 1980; Cameron et al., 1980); they consist of increases in frequency and bandwidth of the C–H modes and are indicative of the introduction of a high degree of conformational and motional disorder into the acyl chains. From the similarity of the changes observed at T_h, we conclude that the formation of the H_{II} phase results in the introduction of additional conformational disorder and an overall increase in the "fluidity" of the acyl chains. This is in agreement with the conclusions reached by ^2H NMR for the acyl chains in dielaidoyl-PE (Galley et al., 1980).

The changes observed in the C=O stretching band reflect its complex structure, comprised of two principal components. The band provides the best indicator of the transition to the inverted hexagonal phase, as the shifts in frequency and bandwidth at T_h are opposite to those observed in the acyl chain melting transition, T_m. However, further studies are required before conclusions can be reached as to the specific structural changes reflected by the spectral changes in the C=O band. Therefore, we are presently investigating the T_h phase change in dioleyl-PE, a system less complex than egg yolk PE.

Furthermore, we have carried out two experiments specifically directed at modulating T_h. In a first experiment, we have studied the effect of the fatty acid composition on the thermotropic behavior of natural egg yolk PE by using a semisynthetic PE derived from egg yolk PC via a transesterification of the head group. As shown in Table I, the natural and the semisynthetic PE contain similar amounts of saturated (47.7% and 50.4%, respectively) and unsaturated acyl chains (50.3% and 49.6%, respectively); however, the natural PE contains a considerable amount of the highly unsaturated 22:6 component. The thermotropic behavior of the two systems is shown in Figure 7, which gives plots of the temperature dependencies of the symmetric CH_2 stretching bands of the two systems. The reduced degree of unsaturation

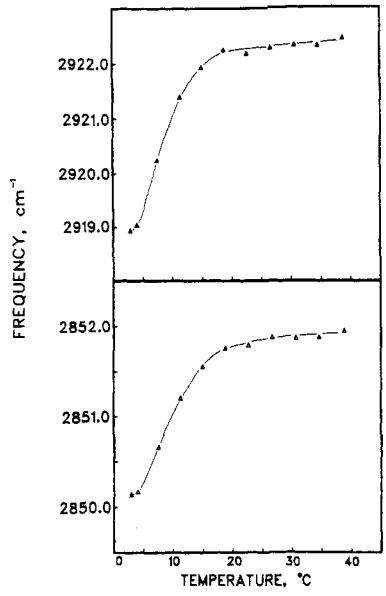

FIGURE 8: Temperature profiles of the symmetric (△) and antisymmetric (▲) CH_2 stretching vibrations of sonicated egg yolk PE.

in the semisynthetic PE results in an increase of the acyl chain melting phase transition temperature by about 8 °C whereas the temperature of the bilayer to nonbilayer phase transition is increased by about 22 °C. Clearly, T_h is much more sensitive to the degree of unsaturation than is T_m, and the formation of the inverted hexagonal phase is favored by unsaturation.

In order to establish whether the transition to the inverted hexagonal phase is affected by the size of the multilamellar dispersions, we have also studied the thermotropic behavior of a sample of natural egg yolk PE that had been subjected to intense sonication (Branson microtip sonicator, 3 × 1 min at 60 W). Figure 8 shows plots of the frequencies of the symmetric and antisymmetric CH_2 stretching bands as a function of temperature. At T_m, the plots show changes characteristic of the acyl chain melting phenomenon; however, no second transition is evident at T_h. While it is difficult to obtain unilamellar PE dispersions (Stollery & Vail, 1977), the sonication results in small vesicles, as evidenced by the large decrease in the light scattered at 400 nm by this preparation. We have not determined the morphological structure of the species formed by sonication; however, there was no TLC evidence of degradation of the PE.

From the present infrared spectroscopic results and a consideration of literature data, it is possible to reach some conclusions regarding the factors which trigger this bilayer to nonbilayer phase transition. If we compare the nature of the molecular packing in the liquid-crystalline and in the inverted hexagonal phases, it is evident that there are substantial differences, particularly in the hydrophobic regions of these structures. The degree of conformational disorder permitted in the liquid-crystalline phase is limited by the constraint that a continuous bilayer surface be maintained. In particular, this restricts the average number of gauche conformers near the head group and requires that the acyl chains adopt a cross-sectional area in the plane of the bilayer surface no larger than that occupied by the head group. These restrictions give rise to the well-known ^2H NMR order plateau which has been observed in a variety of synthetic and natural membranes (Seelig & Seelig, 1974; Stockton et al., 1977) and has also been demonstrated in a statistical mechanical model (Gruen, 1980).

In the inverted hexagonal phase, a much higher population of gauche conformers can be accommodated while a continuous head-group surface is still being maintained. In fact, in order to adopt this packing, it is necessary that the acyl chains fill in a considerable intertubular space. Consequently, we consider that the bilayer to nonbilayer phase transition is triggered by an increase in the population of gauche conformers to the point where the head-group–head-group interactions are no longer sufficient to maintain the multilamellar structure. At this point, the acyl chains "wedge" each other apart while the head-group interaction is largely retained, thus forcing the lipids into the inverted hexagonal phase.

We envisage the inverted tubular H_{II} structure as being formed from adjacent halves of two neighboring bilayers. When the phase change is triggered, the head groups move together as indicated in Figure 9, thus trapping the interbilayer water in the interior of the tube. This model agrees with a pictorial description of the H_{II} phase transition proposed by Cullis & Hope (1978), who have considered the significance of the H_{II} phase as a mechanism for cell fusion and transbilayer transport.

This relatively simple explanation of the factors governing the T_h transition can be related to most of the known facts regarding this transition. First, as shown in this and in all previous studies, the transition to the H_{II} phase always occurs from the conformationally disordered liquid-crystalline phase; to our knowledge, there are no reports of such a transition from the conformationally ordered gel phase. The concept of the conformational disorder of the acyl chains being the driving factor is clearly supported in the comparison between the natural and semisynthetic PE described earlier in this study. The lower transition temperature of the natural PE results from the high proportion of the 22:6 component; these acyl chains promote a high degree of conformational disorder due to their inability to pack regularly and to promote interchain interactions. The conformational disorder in the 18:1 and 18:2 chains is considerably more localized, as demonstrated in recent ^2H NMR studies (Rance et al., 1980).

For a given system with a relatively small head group (such as in PE) and with a certain minimal proportion of unsaturated acyl chains, an increase in temperature is sufficient to trigger

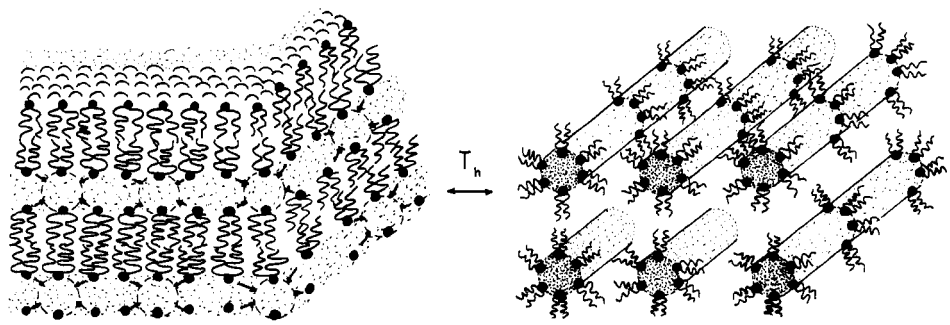

FIGURE 9: Model for the reversible phase change T_h.

this transition by introducing the additional conformational disorder in the acyl chains. Such a conclusion is supported by the very low enthalpy change associated with this dramatic structural rearrangement (Cullis & de Kruiff, 1978). Further support comes from a ^2H NMR study which showed that an increase in temperature beyond T_m in PC leads to the introduction of additional conformational disorder near the head group (Seelig & Seelig, 1974).

So far, only PE, monoglucosyl diglyceride, phosphatidic acid, and cardiolipin have been found to form inverted hexagonal phases, the latter two requiring the presence of Ca^{2+} ions; this phase has not been observed for PC or PS. An excellent review on this subject has been published by Cullis & de Kruiff (1979). The principal differences between these lipids lie in the area occupied by the head group at the bilayer surface. The PC head group is known to occupy a larger area than the head group in PE (McIntosh, 1980), resulting in the substantially greater angle of tilt in the gel phase of PC compared to that in the gel phase of PE. In terms of our hypothesis, the inability of PC to form the inverted hexagonal phase, even if highly unsaturated acyl chains are present, results from the capability of this head group to accommodate a higher population of gauche conformers in the bilayer, due to its greater cross-sectional area.

Thus, although the presence of unsaturated acyl chains is necessary, it is not sufficient for producing the bilayer to nonbilayer phase change, and a relatively small head group is also required. Cardiolipin may also be regarded as having a "small" head group, especially when one considers that it has to accommodate four acyl chains. Also, the glycolipid diglucosyl diglyceride, which has a bulkier head group than monoglucosyl diglyceride, does not form the inverted hexagonal phase (Wieslander et al., 1978). The structures formed by lipids thus represent a delicate balance between the requirements of the acyl chains and those of the head groups.

Studies of mixed lipid systems demonstrate that the addition of PC and PS to PE stabilizes the bilayer structure (Cullis & de Kruiff 1979), as does the addition of the local anesthetic dibucaine (Cullis & Verkleij, 1979). The mechanism of stabilization in this case could be related to the promotion of a larger bilayer area per acyl chain, which thus can accommodate a higher population of gauche conformers per acyl chain. The structurally related local anesthetics procaine and tetracaine have been shown to bind to the bilayer such that they are partially embedded in the hydrophobic region of the bilayer, close to the head group (Boulanger et al., 1980). Consequently, when the surface area of the bilayer is expanded, they increase the volume available for additional gauche conformers close to the bilayer surface.

In contrast, addition of cholesterol has been shown to decrease the stability of the bilayer while promoting the formation of the hexagonal phase (Cullis et al., 1978b). In this case, cholesterol extends deep into the hydrophobic region of the bilayer and effectively reduces the ability of the bilayer to accommodate additional gauche conformers. This latter phenomenon has indeed been observed in PC/cholesterol systems (Stockton & Smith, 1976; Umemura et al., 1980).

In a recent study, Wieslander et al. (1980) have correlated the lipid bilayer stability in *Acholeplasma laidlawii* membranes to the molecular shape of the individual lipid classes, following an approach outlined earlier by Israelachvili et al. (1977). These authors have shown that an increase in the number of cis double bonds, an increase in temperature, and the presence of cholesterol all destabilize the lamellar structure and that the *A. laidlawii* cells compensate for this by changing the composition of the polar head groups. Their general arguments regarding the importance of the relative volumes occupied by the head groups and the acyl chains are in accord with the points made in our discussion and strongly support our model for the bilayer to nonbilayer phase transition.

Finally, we wish to mention that, while unsaturation certainly promotes formation of the inverted hexagonal phase, it may not necessarily be required for the bilayer to nonbilayer phase transition, provided a high population of gauche conformers near the head group could be achieved by other means.

Conclusions

In the present study, we have attempted to probe some of the structural and dynamic properties of aqueous egg yolk PE dispersions. We have used various infrared spectroscopic parameters to detect temperature-induced spectral changes of individual functional groups, located at discrete positions of the PE molecule. The changes in frequency and width of these infrared absorption bands reflect changes in the conformation and rate of motion of the vibrating moiety. Two phase transitions were monitored in this system, a bilayer to bilayer phase transition centered at 12 °C (T_m), and a bilayer to nonbilayer phase (H_{II}) transition centered at 28 °C (T_h). The spectral changes observed in the acyl chain bands at T_m are indicative of a transition from a conformationally and motionally ordered gel phase to a disordered liquid-crystalline phase containing a high population of gauche conformers. There are also considerable changes in the relative intensities of the carbonyl bands at T_m, while changes in the phosphate bands are minimal. The spectral changes at T_h are indicative of the introduction of additional conformational and motional disorder into the acyl chains. While the transition to the H_{II} phase is promoted by an increase in the degree of unsaturation, it is not observed in sonicated PE. The transition T_m is not affected by the sonication and is less sensitive to the fatty acid composition. On the basis of the spectral changes at T_m and T_h, we propose that the bilayer to nonbilayer phase transition results from the fact that the bilayer structure is no longer able to accommodate the simulataneous requirements of a continuous head-group surface and the volume required by the highly disordered acyl chains, the driving force being the introduction of additional conformational disorder into the already disordered liquid-crystalline bilayer phase.

Acknowledgments

We are grateful to Dr. Ian C. P. Smith and Michael G. Taylor for helpful discussions and help with the synthesis of the semisynthetic PE.

References

Akutsu, H., Kyogoku, Y., Nakahara, H., & Fukuda, K. (1975) *Chem. Phys. Lipids 15*, 222.

Boulanger, Y., Schreier, S., Leitch, L. C., & Smith, I. C. P. (1980) *Can. J. Biochem. 58*, 986.

Bush, S. F., Levin, H., & Levin, I. W. (1980) *Chem. Phys. Lipids 27*, 101.

Cameron, D. G., Casal, H. L., & Mantsch, H. H. (1979) *J. Biochem. Biophys. Methods 1*, 21.

Cameron, D. G., Casal, H. L., & Mantsch, H. H. (1980) *Biochemistry 19*, 3665.

Casal, H. L., Cameron, D. G., Smith, I. C. P., & Mantsch, H. H. (1980) *Biochemistry 19*, 444.

Cullis, R. P., & de Kruiff, B. (1976) *Biochim. Biophys. Acta 436*, 523.

Cullis, R. P., & de Kruiff, B. (1978) *Biochim. Biophys. Acta 513*, 31.

Cullis, R. P., & Hope, M. J. (1978) *Nature (London) 271*, 672.
Cullis, R. P., & de Kruiff, B. (1979) *Biochim. Biophys. Acta 559*, 399.
Cullis, R. P., & Verkleij, A. J. (1979) *Biochim. Biophys. Acta 552*, 546.
Cullis, R. P., Verkleij, A. J., & Ververgaert, P. H. J. (1978a) *Biochim. Biophys. Acta 513*, 11.
Cullis, R. P., van Dijck, P. W. M., de Kruiff, B., & de Gier, J. (1978b) *Biochim. Biophys. Acta 513*, 21.
Fookson, J., & Wallach, D. F. H. (1978) *Arch. Biochem. Biophys. 189*, 195.
Gally, H. U., Pluschke, G., Overath, P., & Seelig, J. (1980) *Biochemistry 19*, 1638.
Gruen, D. W. R. (1980) *Biochim. Biophys. Acta 595*, 161.
Israelachvili, J. N., Mitchell, D. J., & Ninham, B. W. (1977) *Biochim. Biophys. Acta 470*, 185.
Kauppinen, J., Karkkainen, T., & Kyro, E. (1978) *J. Mol. Spectrosc. 71*, 15.
Kauppinen, J., Moffatt, D. J., Mantsch, H. H., & Cameron, D. G. (1981) *Appl. Spectrosc.* (in press).
Luzatti, V., Gulik-Krzywicki, T., & Tardieu, A. (1968) *Nature (London) 218*, 1031.
Mantsch, H. H., Cameron, D. G., Umemura, J., & Casal, H. L. (1980) *J. Mol. Struct. 60*, 263.
McIntosh, T. J. (1980) *Biophys. J. 29*, 237.
Rance, M., Jeffrey, K. R., Tulloch, A. P., Butler, K. W., & Smith, I. C. P. (1980) *Biochim. Biophys. Acta 600*, 245.
Rand, R. D., Tinker, D. O., & Fast, P. G. (1971) *Chem. Phys. Lipids 6*, 333.
Seelig, A., & Seelig, J. (1974) *Biochemistry 13*, 4839.
Seelig, J., & Gally, H.-U. (1976) *Biochemistry 15*, 5199.
Stockton, G. W., & Smith, I. C. P. (1976) *Chem. Phys. Lipids 17*, 251.
Stockton, G. W., Johnson, K. G., Butler, K. W., Tulloch, A. P., Boulanger, Y., Smith, I. C. P., Davis, J. H., & Bloom, M. (1977) *Nature (London) 269*, 267.
Stollery, J. G., & Vail, W. J. (1977) *Biochim. Biophys. Acta 471*, 372.
Taylor, M. G., & Smith, I. C. P. (1981) *Chem. Phys. Lipids 28*, 119.
Umemura, J., Cameron, D. G., & Mantsch, H. H. (1980) *Biochim. Biophys. Acta 601*, 999.
Wieslander, A., Ulmius, J., Lindblom, G., & Fontell, K. (1978) *Biochim. Biophys. Acta 512*, 241.
Wieslander, A., Cristiansson, A., Rilfors, L., & Lindblom, G. (1980) *Biochemistry 19*, 3650.
Yang, S. F., Freev, S., & Benson, A. A. (1967) *J. Biol. Chem. 242*, 477.

Purification of Stabilized Band 3 Protein of the Human Erythrocyte Membrane and Its Reconstitution into Liposomes†

Michael F. Lukacovic,* Maurice B. Feinstein, Ramadan I. Sha'afi, and Sherry Perrie

ABSTRACT: The red cell membrane protein, identified on gel electrophoresis as band 3, has been implicated with anion transport. We report here a new rapid procedure for obtaining a stable, functional band 3, essentially free from all other membrane proteins. Red cell ghosts were washed with isotonic saline and solubilized overnight in 0.5% Triton X-100. This extract was applied to a DEAE-cellulose column, and bands 3 and 4.2 and glycophorin (PAS-1) were eluted with high salt concentration. This high-salt fraction was applied to a [[*p*-(chloromercuri)benzamido]ethyl]agarose 4B gel (synthesized according to a modification of the method of Cuatrecasas [Cuatrecasas, P. J. (1971) *Methods Enzymol. 22*, 345–378]) which removed glycophorin and some band 4.2. Pure band 3 was eluted with 0.1 mM cysteine after a low-salt wash. Addition of 15 mM mercaptoethanol immediately after elution was found to prevent protein aggregation. Preparations routinely containing at least 95% band 3 (~1% dimer) and less than 1.5% band 4.2 have been obtained. It should also be noted that this affinity gel can be used to isolate pure glycophorin. Band 3, according to sedimentation analysis on sucrose gradients, existed as a dimer in buffer from which Triton was removed and as a mixture of monomer and dimer in excess Triton. After removal of Triton, band 3 incorporated into liposomes composed of 96% phosphatidylcholine and 4% phosphatidic acid increased sulfate efflux more than 70-fold over that of the control. When 10 μM 4,4′-diisothiocyano-2,2′-stilbenedisulfonate was added to the outside of band 3 containing liposomes, 30–40% of the efflux was inhibited. When the inhibitor was added to the protein before incorporation, nearly complete inhibition was attained. When transport was carried out with no external transportable anions, sulfate efflux was markedly reduced. Influx into liposomes containing band 3 was measured, and a turnover number was calculated which was 24% of the value found for the intact red cell. When stored in 15 mM mercaptoethanol, band 3 remained functional and monomeric for at least a week.

The evidence implicating band 3 of the human erythrocyte membrane as the anion-exchange protein is quite substantial (Knauf, 1979). An important part of this proof has been the isolation and reconstitution of this protein into liposomes and the subsequent demonstration of its ability to mediate anion transport (Rothstein et al., 1975; Ross & McConnell, 1977, 1978). Several laboratories have accomplished this; however, the band 3 preparations in each case have been contaminated with other membrane proteins, notably bands 4.2 and 4.5 and glycophorin (PAS-1). An additional problem has been that isolated band 3 preparations are notoriously unstable and rapidly form high molecular weight aggregates (Yu & Steck,

† From the Departments of Pharmacology (M.F.L., M.B.F., and S.P.) and Physiology (R.I.S.), University of Connecticut Health Center, Farmington, Connecticut 06032. *Received June 3, 1980.* This work was supported by U.S. Public Health Service Grants GM-17536 and HL24160.

* Address correspondence to this author at the Biophysical Laboratory, Harvard Medical School, Boston, MA 02115. Material described herein was submitted as part of a thesis in partial fulfillment of the requirements for the degree of Doctor of Philosophy in Pharmacology.

0006-2960/81/0420-3145$01.25/0